Cement and Concrete Research 41 (2011) 1095–1103

Contents lists available at ScienceDirect

Cement and Concrete Research

journal homepage: http://ees.elsevier.com/CEMCON/default.asp

Calculation of chloride concentration at color change boundary of $AgNO_3$ colorimetric measurement

Fuqiang He [a], Caijun Shi [b,*], Qiang Yuan [c], Xiaopeng An [b], Baihui Tong [b]

[a] Department of Civil Engineering and Architecture, Xiamen University of Technology, Xiamen 361024, PR China
[b] Key Laboratory of Building Safety and Energy Efficiency (Ministry of Education), College of Civil Engineering, Hunan University, Changsha 410082, PR China
[c] School of Civil Engineering, Central South University, Changsha 410075, PR China

ARTICLE INFO

Article history:
Received 4 August 2010
Accepted 21 June 2011

Keywords:
Concrete E
Chloride D
Transport property

ABSTRACT

$AgNO_3$ colorimetric measurement of chloride in cement-based materials can be implemented owing to chemical reactions between Ag^+ and Cl^- or OH^- ions, which result in the precipitation of AgCl and Ag_2O. When the mass ratio of AgCl to precipitated AgCl + Ag_2O reaches a critical value ($P_{crit\text{-}AgCl}$), a color change boundary appears. In this paper, chloride concentrations required for the formation of the critical mass ratio of AgCl to precipitated AgCl + Ag_2O derived from the $AgNO_3$–NaCl–NaOH system were calculated based on the solubility products of silver hydroxide and silver chloride, and mass conservation of the chemical reactions. $P_{crit\text{-}AgCl}$ was determined as 0.65 through a series of $AgNO_3$ colorimetric measurements on cement-based materials. Calculated results indicated that if Ag^+ could react with all OH^- and Cl^-, there existed a linear relationship between the critical chloride concentration for color change ($C_{crit\text{-}Cl^-}$) and OH^- concentration (C_{OH^-}), namely $C_{crit\text{-}Cl^-} = 1.6C_{OH^-}$. If Ag^+ could react with only partial OH^- and Cl^-, there existed an exponential relationship among $C_{crit\text{-}Cl^-}$ and C_{OH^-}, Ag^+ concentration (C_{Ag^+}), volume of $AgNO_3$ solution (V_{Ag^+}) as well as the volume of NaCl + NaOH solution ($V_{OH^- + Cl^-}$), namely $C_{crit\text{-}Cl^-} = 0.00695C_{OH^-} + 0.608C_{Ag^+}V_{Ag^+}/V_{OH^- + Cl^-}$. It can be concluded that the alkalinity of cement-based materials, concentration and volume of sprayed $AgNO_3$ solution and volume of pore solution have effects on chloride concentration at the color change boundary (C_d). Calculated C_d values ranged between 0.03 and 0.96 mol/L (in pore solution) or 0.011% to 2.27% (by the mass of binder), respectively. This explains why reported range of chloride concentration at the color change boundary in publications varied in a broad range.

1. Introduction

The $AgNO_3$ colorimetric method is a quick and easy method to measure the free chloride penetration depth in cement-based materials [1–4]. In this method, an $AgNO_3$ solution (normally 0.1 mol/L) is sprayed onto freshly fractured surface of cement-based materials. The area containing high chloride concentration turns silvery white due to the formation of AgCl derived from the reaction between Ag^+ and Cl^-. The area containing low concentration of chloride or no chloride turns into brown due to the formation of Ag_2O from the reactions between Ag^+ and OH^-. The color change boundary is not really the boundary of zones containing chloride and no chloride, but a curve close to the actual penetration front of chloride [5–8]. In the $AgNO_3$ colorimetric method, color change depth X_d refers to the average distance between the chloride-exposed surface and the color change boundary.

The $AgNO_3$ colorimetric method involves two parameters, X_d and chloride concentration at the color change boundary (C_d). X_d and C_d have been widely used for measuring chloride migration in cement-based materials. In NordTest NT Build 492 [9], a 0.1 mol/L $AgNO_3$ solution is used to measure the "chloride penetration depth" after the electrical migration testing; both X_d and C_d are used to calculate non-steady-state migration coefficient of chloride (D_{nssm}). Baroghel-Bouny et al. [5,6,10] used X_d and C_d to calculate apparent chloride diffusion coefficient (D_{app}) of concrete exposed to chloride environments. When D_{nssm} and D_{app} were calculated [5,6,9,10], C_d value of 0.07 mol/L was used as suggested by Tang [11]. For existing concrete structures, periodical spraying of $AgNO_3$ solution can be easily performed to obtain a series of X_d with time, which can provide the kinetic process of chloride penetration. This information can be useful for the assessment of the chloride corrosion risk of existing concrete structures [5,6,12] or for monitoring the residual life prediction of existing concrete structures [13,14].

Many researchers have studied C_d and noticed that it varied within a broad range. They expressed C_d with three different forms: free chloride concentration (in pore solution), water soluble chloride contents (by the mass of binder), and total chloride concentration (by the mass of binder). It was found that free chloride concentration ranged between 0.071 and 0.714 mol/L [7,15], water soluble chloride contents from 0.01 to 1.69% [4–6,12,15–17], and the total chloride concentration from 0.2 to 1.5% [4–6,15,18,19].

---

[*] Corresponding author. Tel./fax: +86 731 8882 3937.
E-mail address: cshi@hnu.edu.cn (C. Shi).

0008-8846/$ – see front matter © 2011 Elsevier Ltd. All rights reserved.
doi:10.1016/j.cemconres.2011.06.008

As shown above, in some cases, the measured C_d is far higher than 0.07 mol/L as used for the calculation of D_{nssm} in NT build492 [9] and D_{app} used in publications [5,6,10], or the critical chloride concentration for the initiation of corrosion of steel in concrete as reported in many publications [20]. The use of a single value instead of actual concentrations may result in significant error in calculated D_{nssm} and D_{app}, the kinetics of chloride penetration process and chloride corrosion risk assessment of existing concrete structures. The purpose of this study was to clarify those factors influencing the chloride concentration at the color change boundary and to determine its range, so as to better apply the $AgNO_3$ colorimetric method.

2. Calculations of precipitation

2.1. Theoretical base for calculation

There mainly exist Ca^{2+}, Na^+, K^+, OH^-, Cl^- and SO_4^{2-} in pore solution of hydrated cement materials exposed to chloride. Among them, OH^-, Cl^- and SO_4^{2-} can react with Ag^+ in sprayed $AgNO_3$ solution. The reactions can be expressed as follows:

$$Ag^+ + Cl^- \rightarrow AgCl\downarrow(\text{Silvery white, solubility product } 1.8 \times 10^{-10} \text{at } 25^\circ C)$$

$$Ag^+ + OH^- \rightarrow AgOH \rightarrow Ag_2O\downarrow(\text{Brown, solubility product } 2.6 \times 10^{-8} \text{at } 25^\circ C)$$

$$Ag^+ + SO_4^{2-} \rightarrow Ag_2SO_4\downarrow(\text{White, solubility product } 1.2 \times 10^{-5} \text{at } 25^\circ C)$$

Analyses showed that there is a little SO_4^{2-} in pore solution of hydrated cement-based materials [21]. Concentrations of OH^- and SO_4^{2-} in pore solutions of cement-based materials with silica fume, fly ash and slag powder change in the ranges of 0.1–18.2 and 18–360 mmol/L, respectively. Concentration ratio of OH^- to SO_4^{2-} is from 25 to 180. Additionally, solubility products of AgCl and Ag_2O are much higher than that of $AgSO_4$. When Ag^+, OH^-, Cl^- and SO_4^{2-} present together in solution, Ag^+ reacts first with Cl^-, second with OH^- and last with SO_4^{2-}. Associated with very low concentration of SO_4^{2-} ions, the reaction between Ag^+ and SO_4^{2-} could be ignored.

He et al. [7,22] added $AgNO_3$ solution with different concentrations into solutions containing different concentrations of NaCl and NaOH, and noticed that both AgCl and Ag_2O would precipitate. When AgCl content in the mixed precipitates ($AgCl + Ag_2O$) reached a certain critical value ($P_{crit\text{-}AgCl}$), the color of the precipitates started to change from brown to gray. In this study, Cl^- concentration corresponding to $P_{crit\text{-}AgCl}$ is called as chloride concentration for color change of the precipitates, $C_{crit\text{-}Cl^-}$.

In the $AgNO_3$–NaOH–NaCl system, the mass ratio of AgCl to the mixed precipitates ($AgCl + Ag_2O$) can be theoretically calculated based on the solubility products of silver hydroxide and silver chloride, and mass conservation of the chemical reactions as follows:

Solubility product of silver hydroxide:

$$C_{a-Ag^+} \times C_{a-OH^-} = 2.6 \times 10^{-8} \tag{1}$$

Solubility product of silver chloride:

$$C_{a-Ag^+} \times C_{a-Cl^-} = 1.8 \times 10^{-10} \tag{2}$$

Mass conservation of the reactions:

$$V_{Ag^+}C_{Ag^+} - V_T C_{a-Ag^+} = V_{OH^-+Cl^-}C_{Cl^-} - V_T C_{a-Cl^-} + V_{OH^-+Cl^-}C_{OH^-} - V_T C_{a-OH^-} \tag{3}$$

where: C_{Ag^+}, C_{Cl^-} and C_{OH^-} are the mole concentrations of Ag^+, Cl^- and OH^- before the reactions. $C_{a\text{-}Ag^+}$, $C_{a\text{-}Cl^-}$ and $C_{a\text{-}OH^-}$ are the mole concentrations of Ag^+, Cl^- and OH^- after the reactions. V_{Ag^+} is the volume of $AgNO_3$ solution added to the NaOH + NaCl solution, $V_{OH^-} + {}_{Cl^-}$ is volume of NaOH + NaCl solution, V_T is the total volume of mixed solution.

When the equivalents of $AgNO_3$ added were the same as those of NaCl in the NaOH + NaCl solution, or $C_{Ag^+} = C_{Cl^-}$, there was a good agreement between the calculated and the measured values [22]. However, in most cases, the Cl^- in the pore solution of concrete is varying and will only be equivalent to $AgNO_3$ sprayed onto concrete in a limited region. The mass ratio of AgCl (P_{AgCl}) to the mixed precipitates ($Ag_2O + AgCl$) can be calculated by Eq. (4). In association with Eqs. (1), (2) and (3), the $C_{crit\text{-}Cl^-}$ values for different concentrations of $AgNO_3$, NaCl and NaOH can be obtained.

$$P_{AgCl} = \frac{(V_{OH^- + Cl^-}C_{Cl^-} - V_T C_{a-Cl^-})m_{AgCl}}{(V_{OH^- + Cl^-}C_{Cl^-} - V_T C_{a-Cl^-})m_{AgCl} + \frac{(V_{OH^- + Cl^-}C_{OH^-} - V_T C_{a-OH^-})}{2}m_{Ag_2O}} \tag{4}$$

where: m_{AgCl} is the molecular mass of AgCl; m_{Ag2O} is the molecular mass of Ag_2O. When P_{AgCl} reaches the critical value $P_{crit\text{-}AgCl}$, C_{Cl^-} in Eqs. (3) and (4) can be regarded as $C_{crit\ Cl^-}$.

2.2. Calculation range and critical parameters

Considering the alkalinity range of cement-based materials and the actual possible volume ratios of sprayed $AgNO_3$ solution to pore solution, the ranges of these parameters for the calculation of $C_{crit\text{-}Cl^-}$ by using Eqs. (1), (2), (3) and (4) are listed in Table 1. Two ratios, $R_1(C_{Cl^-}/C_{OH^-})$ and $R_2(V_{Ag^+}/V_{OH^-} + {}_{Cl^-})$, are defined to discuss the trend of chloride concentration at the color change boundary under different conditions. The critical values for R_1, R_2, C_{Cl^-} and P_{AgCl} are described in Table 2.

2.3. The case of $V_{Ag^+}C_{Ag^+} \geq V_{OH^-} + {}_{Cl^-}C_{OH^-} + V_{OH^-} + {}_{Cl^-}C_{Cl^-}$

By solving Eqs. (1), (2), (3) and (4), a quadratic equation of C_{Cl^-} was obtained as follows:

$$aC_{Cl^-}^2 + bC_{Cl^-} + c = 0. \tag{5}$$

Table 1
Description and range of parameters.

Parameters	Description	Range
C_{OH^-}	OH^- concentration in pore solution of cement-based materials	0.01–0.6
$V_{OH^-} + {}_{Cl^-}/V_{Ag^+}$	Volume ratio of $AgNO_3$ indicator to pore solution taken part in the colorimetric reaction	100–0.0001
C_{Ag^+}	Concentration of sprayed $AgNO_3$ indicator	0.035–0.5
P_{AgCl}	The mass ratio of AgCl ro Ag_2O + AgCl mixed precipitates	0.1–0.9

Table 2
Description of some critical parameters.

Parameter	Description
$R_{1\text{-crit}}$	The least R_1 leading to the color change of the mixed precipitates from brown to silvery or the color change boundary appears
$R_{2\text{-crit}}$	The least R_2 when Ag^+ can react with all Cl^- and OH^-
$C_{crit\ Cl^-}$	The least Cl^- concentration leading to the color change of the mixed precipitates from brown to silvery or the color change boundary appears
$P_{crit\text{-}AgCl}$	The least P_{AgCl} leading to the color change of the mixed precipitates from brown to silvery or the color change boundary appears

Considering $C_{Cl^-}>0$, solution of Eq. (5) can be expressed as follows:

$$C_{Cl^-} = \frac{-b+\sqrt{b^2-4ac}}{2a} \qquad (6)$$

a, b and c in Eq. (6) are listed as follows:

$$a = \left(k_{spAgOH}/k_{spAgCl}+1\right)V_T\Delta_3^2/\Delta_1^2 - V_{OH^- - Cl^-}\Delta_3/\Delta_1 \qquad (7)$$

$$b = C_{Ag^+}V_{Ag^+}\Delta_3/\Delta_1 + V_{OH^- - Cl^-}\Delta_2/\Delta_1 - V_{OH^- - Cl^-}C_{OH^-}/\Delta_1 - 2\left(k_{spAgOH}/k_{spAgCl}+1\right)V_T\Delta_2\Delta_3/\Delta_1^2 \qquad (8)$$

$$c = \left(k_{spAgOH}/k_{spAgCl}+1\right)V_T\Delta_2^2/\Delta_1^2 + V_{OH^- - Cl^-}C_{OH^-}\Delta_2/\Delta_1 - C_{Ag^+}V_{Ag^+}\Delta_2/\Delta_1 - k_{spAgCl}. \qquad (9)$$

In Eqs. (7)–(9), units of a, b and c are L, mol and mol^2/L, respectively. Δ_1, $\Delta_2$and Δ_3 are given in Eqs. (10)–(12). Their units are L, mol and L, respectively.

$$\Delta_1 = 2\left(V_T m_{AgCl} - P_{AgCl}m_{AgCl}V_T\right) - k_{spAgOH}P_{AgCl}m_{Ag_2O}V_T/k_{spAgCl} \qquad (10)$$

$$\Delta_2 = P_{AgCl}m_{Ag_2O}V_{OH^- - Cl^-}C_{OH^-} \qquad (11)$$

$$\Delta_3 = 2m_{AgCl}\left(1-P_{AgCl}\right)V_{OH^- - Cl^-} \qquad (12)$$

where: k_{spAgCl} and k_{spAgOH} are solubility products of AgCl and Ag_2O, and equal to 1.8×10^{-10} and 2.6×10^{-8}, respectively.

In the case of $V_{Ag^+}C_{Ag^+}\geq V_{OH^-+Cl^-}C_{OH^-}+V_{OH^-+Cl^-}C_{Cl^-}$, V_{Ag^+}, C_{Ag^+}, $V_{OH^-+Cl^-}$, C_{OH^-}, P_{AgCl} and solubility products of AgCl and Ag_2O (k_{spAgCl} and k_{spAgOH}) were input as parameters to obtain a, b and c, Eq. (6) with different a, b and c can be solved to get different C_{Cl^-} values.

Relationships between C_{OH^-} and C_{Cl^-} at $P_{AgCl}=0.6$ and 0.8 are shown in Fig. 1, respectively. It can be seen that, for a given P_{AgCl}, when $V_{Ag^+}C_{Ag^+}\geq V_{OH^-+Cl^-}C_{OH^-}+V_{OH^-+Cl^-}C_{Cl^-}$, C_{Cl^-} needed for the precipitation of AgCl is linearly dependent upon C_{OH^-}. Fitted R_1 values for different P_{AgCl} values are given in Table 3. As can be seen from Table 3, C_{Cl^-} needed for the precipitation of AgCl is linearly dependent upon C_{OH^-} when P_{AgCl} is from 0.1 to 0.9.

Relationship between R_1 and P_{AgCl} is plotted in Fig. 2. It can be seen from Fig. 2 that there is a very good exponential correlation between R_1 and P_{AgCl}, namely:

$$R_1 = 0.0077e^{7.55P_{AgCl}} + 0.3. \qquad (13)$$

Table 3
Fitted R_1 values at different P_{AgCl} values.

P_{AgCl}	0.1	0.2	0.3	0.4	0.5	0.6	0.65	0.7	0.75	0.8	0.9
R_1	0.09	0.2	0.35	0.54	0.81	1.21	1.5	1.89	2.42	3.23	7.27
R^2	1	1	1	1	1	1	1	1	1	1	1

From the definition of $R_1=(C_{Cl^-}/C_{OH^-})$, Eq. (13) can be rewritten as follows:

$$C_{Cl^-} = \left(0.0077e^{7.55P_{AgCl}} + 0.3\right)C_{OH^-}. \qquad (14)$$

When $P_{AgCl}=P_{crit\text{-}AgCl}$, the chloride concentration for the color change or at the color change boundary of the colorimetric measurement of cement-based materials can be expressed as follows:

$$C_{Cl^-} = \left(0.0077e^{7.55P_{crit-AgCl}} + 0.3\right)C_{OH^-} \qquad (15)$$

The range of $P_{crit\text{-}AgCl}$ can be determined based on a series of experiments (as discussed in Section 3). When the amount of sprayed $AgNO_3$ is sufficient to react with all OH^- and Cl^- ions in the pore solution at the color change boundary, the chloride concentration at color change boundary depends only on the alkalinity of cement-based materials.

2.4. The case of $V_{Ag^+}C_{Ag^+}<V_{OH^-+Cl^-}C_{OH^-}+V_{OH^-+Cl^-}C_{Cl^-}$

In the case of $V_{Ag^+}C_{Ag^+}<V_{OH^-+Cl^-}C_{OH^-}+V_{OH^-+Cl^-}C_{Cl^-}$, V_{Ag^+}, C_{Ag^+}, $V_{OH^-+Cl^-}$, C_{OH^-}, P_{AgCl} and solubility products of AgCl and Ag_2O (k_{spAgCl} and k_{spAgOH}) were input as parameters to obtain a, b and c, the Eq. (6) with different a, b and c can be solved to get different C_{Cl^-} value.

By analyzing data on C_{OH^-}, R_2 and C_{Cl^-}, it can be found that for given P_{AgCl} and C_{Ag^+}, there are linear relationships among them, which can be written as Eq. (16):

$$C_{Cl^-} = AC_{OH^-} + BR_2. \qquad (16)$$

A is dimensionless and the unit of B is mol/L. A and B values are fitted by regression analysis in excel software and listed in Table 4. It is necessary to point out that all fitted situations have $R^2=1$. It can be seen from Table 4 that A is a constant and B is a variable. Based on data in Table 4, through fitting data P_{AgCl} and B, it can be noticed that there is a linear relationship between B and P_{AgCl}, as shown in Fig. 3, which can be written as Eq. (17):

$$B = MP_{AgCl}. \qquad (17)$$

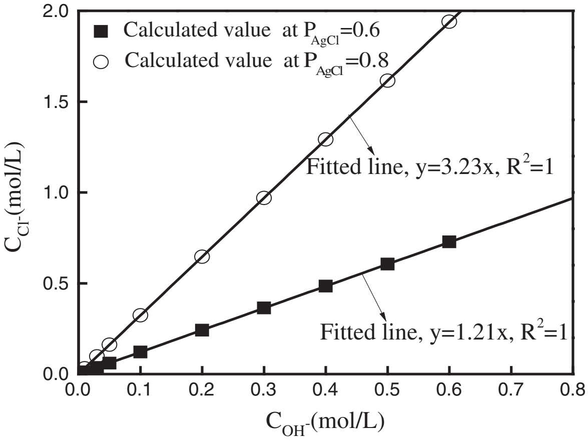

Fig. 1. Relationships between C_{OH^-} and C_{Cl^-} when $P_{AgCl}=0.6$ and 0.8 in the case of $V_{Ag^+}C_{Ag^+}\geq V_{OH^-+Cl^-}C_{OH^-}+V_{OH^-+Cl^-}C_{Cl^-}$.

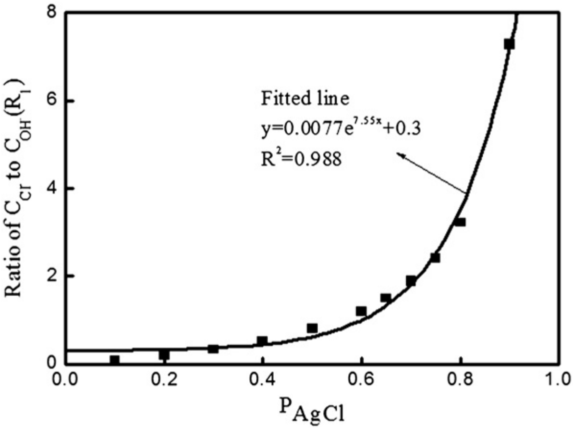

Fig. 2. Relationship between R_1 and P_{AgCl} in the case of $V_{Ag^+}C_{Ag^+}\geq V_{OH^-+Cl^-}C_{OH^-}+V_{OH^-+Cl^-}C_{Cl^-}$.

Table 4
Values for A and B in Eq. (16).

P_{AgCl}	C_{Ag^+} (mol/L)					
	0.5		0.1		0.035	
	A	B	A	B	A	B
0.2	0.00695	0.0812	0.00695	0.0162	0.00695	0.00567
0.3	0.00695	0.138	0.00695	0.0277	0.00695	0.00969
0.4	0.00695	0.173	0.00695	0.0346	0.00695	0.0121
0.5	0.00695	0.231	0.00695	0.0461	0.00695	0.0161
0.6	0.00695	0.272	0.00695	0.0545	0.00695	0.0191
0.7	0.00695	0.323	0.00695	0.0646	0.00695	0.0226
0.8	0.00695	0.381	0.00695	0.0762	0.00695	0.0267
0.9	0.00695	0.415	0.00695	0.083	0.00695	0.0291

The unit of M is mol/L. M values were fitted within the range of C_{Ag^+} which is from 0.035 to 0.5 mol/L. Relationship between fitted M and C_{Ag^+} values is plotted in Fig. 4. As can be seen from the figure, Eq. (18) can be observed.

$$M = 0.922C_{Ag^+}. \tag{18}$$

Constant A in Table 4, Eqs. (17) and (18) were taken into Eq. (16), and thus Eq. (19) can be obtained as:

$$C_{Cl^-} = 0.00695C_{OH^-} + 0.922C_{Ag^+}P_{AgCl}R_2. \tag{19}$$

When P_{AgCl} reaches $P_{crit\text{-}AgCl}$, Eq. (20) was obtained.

$$C_{crit-Cl^-} = 0.00695C_{OH^-} + 0.922C_{Ag^+}P_{crit-AgCl}R_2. \tag{20}$$

It can be seen from Eq. (20) that in the case of $V_{Ag^+}C_{Ag^+} < V_{OH^-+Cl^-}C_{OH^-} + V_{OH^-+Cl^-}C_{Cl^-}$, C_{OH^-} has little effect on $C_{crit\text{-}Cl^-}$. R_2 may change in a relatively large range and thus has a significant effect on $C_{crit\text{-}Cl^-}$. During colorimetric measurement of cement-based materials, the R_2 is the volume ratio of sprayed $AgNO_3$ to pore solution taking part in the colorimetric reactions. However, it is difficult to determine R_2 based on the actual colorimetric measurement of cement-based materials. This will be discussed in Section 4 based on some assumed range of parameters.

2.5. Calculation of $P_{crit\text{-}AgCl}$

Based on Eqs. (1), (2) and (4), Eq. (21) can be derived for the calculation of P_{AgCl}:

$$P_{AgCl} = \frac{1}{1 + \dfrac{0.81(C_{OH^-} - 144(R_2 + 1)C_{a-Cl^-})}{R_1C_{OH^-} - (R_2 + 1)C_{a-Cl^-}}} \times 100\%. \tag{21}$$

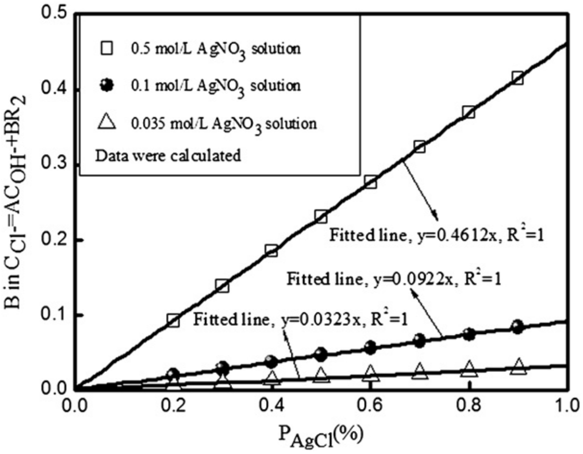

Fig. 3. Relationship between P_{AgCl} and coefficient B in Eq. (16).

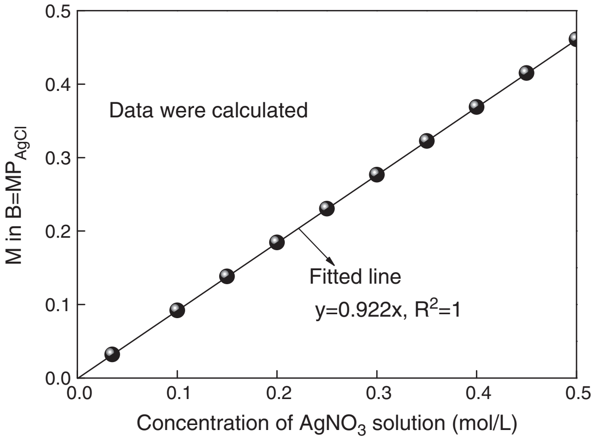

Fig. 4. Relationship between concentration of $AgNO_3$ solution and coefficient M in Eq. (17).

If $V_{Ag^+}C_{Ag^+} = V_{OH^-+Cl^-}C_{OH^-} + V_{OH^-+Cl^-}C_{Cl^-}$, $C_{a\text{-}Cl^-}$ is 1.11×10^{-6} mol/L based on calculations using Eqs. (1) and (2).

When $V_{Ag^+}C_{Ag^+} > V_{OH^-+Cl^-}C_{OH^-} + V_{OH^-+Cl^-}C_{Cl^-}$, $C_{a\text{-}Cl^-}$ will be less than 1.11×10^{-6} mol/L. In this situation, considering ranges of C_{OH^-}, R_1 and R_2, Eq. (22) can be used for calculating P_{AgCl}.

$$P_{AgCl} \approx \frac{C_{Cl^-}}{C_{Cl^-} + 0.81C_{OH^-}}. \tag{22}$$

When $V_{Ag^+}C_{Ag^+} > V_{OH^-+Cl^-}C_{OH^-} + V_{OH^-+Cl^-}C_{Cl}$, if Cl^- and OH^- concentrations can be measured as color changes or color change boundary appears, $P_{crit\text{-}AgCl}$ can be calculated according to Eq. (22).

3. Experimental determination of $P_{crit\text{-}AgCl}$

To determine $P_{crit\text{-}AgCl}$, $AgNO_3$ colorimetric experiments were conducted on cement mortars as follows: seven batches of mortar containing 1.5% NaCl by mass of the binder were cast into PVC moulds with a size of Φ40 × 150 mm. Chemical compositions of various cementitious materials are given in Table 5 and mixing proportions of mortar are listed in Table 6. After demoulding at 24 h age, a layer of mortar about 3 mm thick was cut off without spraying cooling water. The dry-cut surface of the mortar specimens were immediately sprayed with 0.5 and 1.0 mol/L $AgNO_3$ solutions. Use of 0.5 and 1.0 mol/L $AgNO_3$ solutions was to ensure that some extra $AgNO_3$ could still exist after the colorimetric reactions so that Eq. (22) can be used to calculate $P_{crit\text{-}AgCl}$. The cutting and spraying were repeated at 6-hour intervals until the surface could turn into slightly brown at the same time after being sprayed with 0.5 and 1.0 mol/L $AgNO_3$ solutions.

When NaCl is mixed into cement-based materials, it can be regarded that all Cl^- from NaCl are free. The concentration of free chloride in cement-based materials is higher than that which can be detected by $AgNO_3$ colorimetric method at early ages. With the development of hydration, more free chloride in pore solution was bound [16], the color of the dry-cut surfaces turned into gray from silvery white, then into

Table 5
Chemical composition of various cementitious materials *w*/%.

Materials	CaO	SiO_2	Al_2O_3	MgO	SO_3	Fe_2O_3	L O I
Cement	61.79	21.58	4.67	2.48	2.85	2.66	
Silica fume	1.95	90.00		0.27	0.30	0.59	
Fly ash	3.24	47.96	37.72	0.88	0.24	4.58	4.1
Slag powder	36.90	32.18	14.64	9.64	1.66	0.54	

L O I is loss on ignition.

Table 6
OH^- and Cl^- concentrations in pore solution of mortar containing chloride when dry-cutting surface turning into brown after being sprayed with 0.5 and 1.0 mol/L $AgNO_3$ solutions.

Binder composition	Water/binder ratio	Sand/binder ratio	OH^- (mol/L)	Cl^- (mol/L)	$R_{1\text{-crit}}$	$P_{\text{crit-AgCl}}$	Time of turning into brown
100% PC	0.5	2.5	0.29	0.44	1.52	0.653	102 h
95% PC + 5% SF	0.5	2.5	0.26	0.4	1.54	0.656	102 h
85% PC + 15% SF	0.5	2.5	0.23	0.35	1.52	0.653	96 h
80% PC + 20% FA	0.5	2.5	0.25	0.38	1.52	0.653	96 h
60% PC + 40% FA	0.5	2.5	0.26	0.37	1.42	0.637	120 h
70% PC + 30% SL	0.5	2.5	0.29	0.28	0.97	0.545	54 h
40% PC + 60% SL	0.5	2.5	0.28	0.29	1.04	0.563	78 h

brown as mortar curing time increased. The pictures of a dry-cut surface at different ages after being sprayed with $AgNO_3$ solutions are shown in Fig. 5.

To ensure sprayed $AgNO_3$ amount is enough to react with all Cl^- and OH^- in pore solution, about 5 ml $AgNO_3$ solution was carefully sprayed onto 16 cm^2 dry-cutting surfaces without dropping from the surfaces. After about 30 min of natural drying at room temperature, if both dry-cut surfaces sprayed with 0.5 and 1.0 mol/L $AgNO_3$ solutions turned slightly brown, the pore solution of the specimen was expressed out using a special device. The expressed solution was analyzed for Cl^- and OH^- ion concentrations using an automatic potentiometric titrimeter.

The results measured and calculated according to Eq. (22) are listed in Table 6. As can be seen from Table 6, mortar specimens without slag powder demonstrated very similar $R_{1\text{-crit}}$ and $P_{\text{crit-AgCl}}$ values, which are higher than $R_{1\text{-crit}}$ and $P_{\text{crit-AgCl}}$ values of mortar specimens with slag powder. This is possibly because the color of the $AgCl + Ag_2O$ precipitates is also influenced by the color of mortar. As can be seen from Fig. 6, the color of slag mortar specimen is dark blue. When the color of $AgCl + Ag_2O$ precipitates is white, it can be distinguished from the dark blue surface of slag mortar specimen. When the color of $AgCl + Ag_2O$ precipitates becomes slightly brown, it can't be distinguished from the dark blue surface of slag mortar specimen. When color of $AgCl + Ag_2O$ precipitates becomes dark brown, it can only be distinguished from the dark blue surface of slag mortar specimen as slightly brown. In this situation, compared with specimens without slag powder, lower $P_{\text{crit-AgCl}}$ for specimens with slag powder is needed to distinguish the color of the $AgCl + Ag_2O$ precipitates from the color of slag mortar specimens. It can also be seen from Table 6 that different

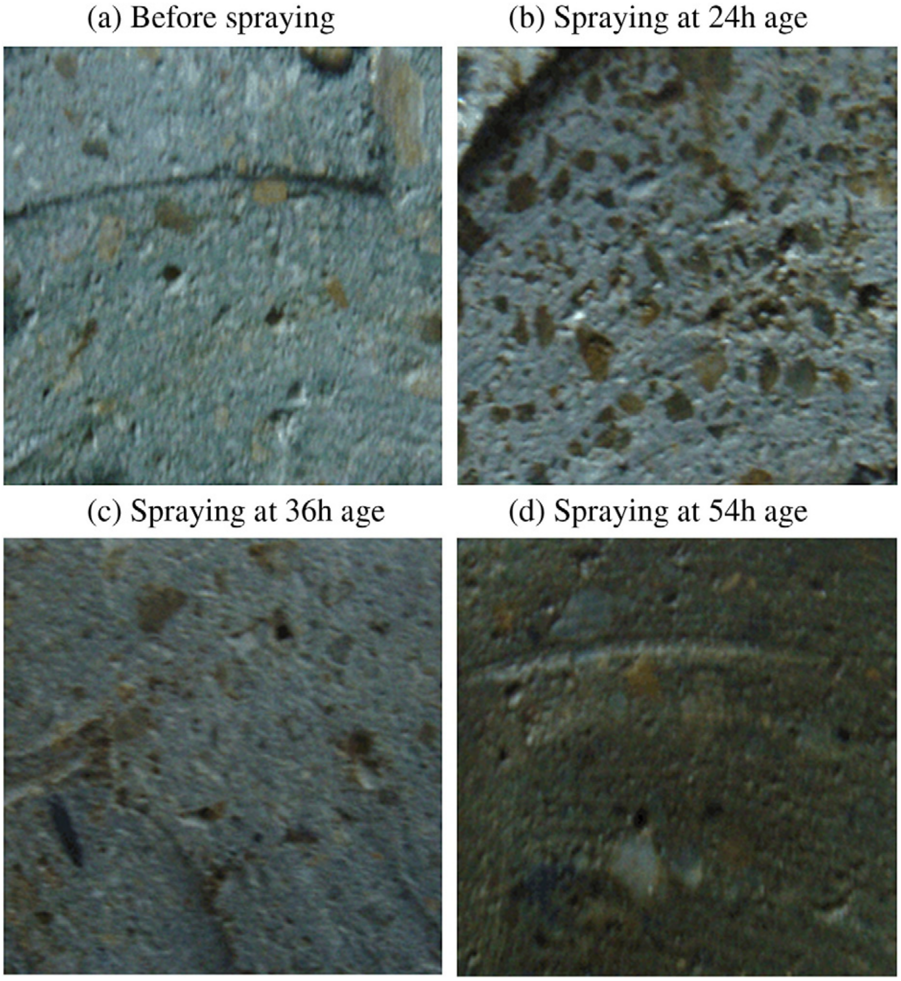

Fig. 5. Typical colorimetric pictures of slag mortars after being sprayed with $AgNO_3$ solution at different times. (a) Before spraying (b) Spraying at 24 h age (c) Spraying at 36 h age (d) Spraying at 54 h age.

(a) OPC mortar specimen (b) Mortar specimen with silica fume

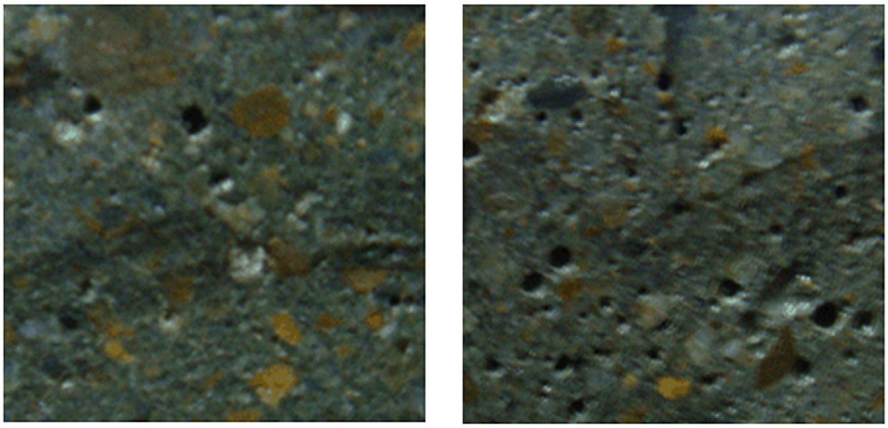

(c) Mortar specimen with fly ash (d) Mortar specimen with slog powder

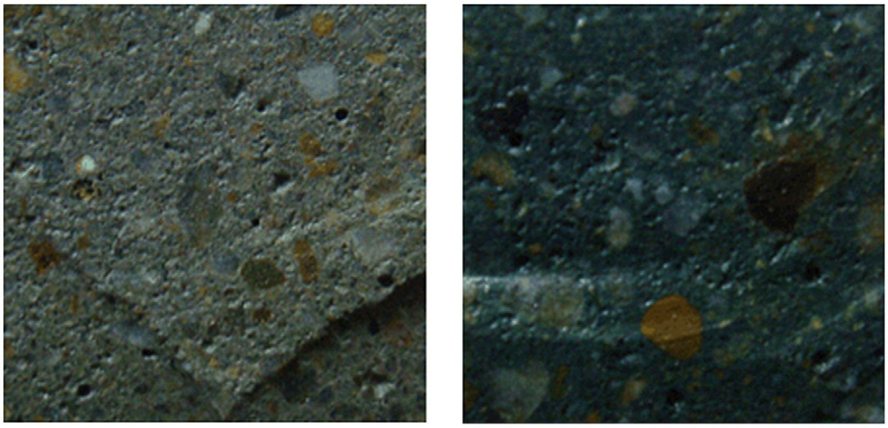

Fig. 6. Pictures of typical cement-based mortar specimens. (a) OPC mortar specimen. (b) Mortar specimen with silica fume. (c) Mortar specimen with fly ash. (d) Mortar specimen with slag powder.

time periods are needed for different specimens turning their colors into slightly brown. This is because different binders have different binding rate and capacity for Cl^- ions. Incorporation of silica fume can decrease binding capacity of the binder, while incorporation of fly ash and slag powder can increase binding capacity of the binder [23–25]. However, it was found from Table 6 that incorporation of 5% and 10% silica fume, and 20% fly ash gave a little change in binding rate of binder, but incorporation of 30% and 60% slag powder, and 40% fly ash (by mass of binder) increased binding rate of binder.

It can also be found from Table 6 that $P_{crit\text{-}AgCl}$ is around 0.55 for mortar specimens with slag powder, and around 0.65 for all other mortars. Since the use of 0.55 or 0.66 for $P_{crit\text{-}AgCl}$ did not cause a significant difference for the calculated $C_{crit\text{-}Cl^-}$ values from Eqs. (15) and (20), 0.65 is used as $P_{crit\text{-}AgCl}$ value for all different mortars for the purpose of simple calculation.

4. Chloride concentration at the color change boundary

4.1. Calculation of $R_{2\text{-}crit}$

When $V_{Ag^+}C_{Ag^+} = V_{OH^-+Cl^-}C_{OH^-} + V_{OH^-+Cl^-}C_{Cl^-}$, R_2 reaches $R_{2\text{-}crit}$, which determines whether Ag^+ can react with all Cl^- and OH^-. $V_{Ag^+}C_{Ag^+} = V_{OH^-+Cl^-}C_{OH^-} + V_{OH^-+Cl^-}C_{Cl^-}$ can be written as Eq. (23):

$$R_{2-crit} = \frac{C_{OH^-} + C_{Cl^-}}{C_{Ag^+}}. \qquad (23)$$

Based on Eqs. (1), (2), (3), (4) and (23), Eq. (24) can be derived as:

$$R_{2-crit} = \frac{\left(1-0.19p_{AgCl}\right)\cdot C_{OH^-} - 1.3\times10^{-4}P_{AgCl} + 1.12\times10^{-6}\left(1-P_{AgCl}\right)}{\left(1-p_{AgCl}\right)\cdot C_{Ag^+} + 1.3\times10^{-4}P_{AgCl} - 1.12\times10^{-6}\left(1-P_{AgCl}\right)}. \qquad (24)$$

When P_{AgCl} gets $P_{crit\text{-}AgCl}$, Eq. (24) can be written as follows:

$$R_{2-crit} = \frac{\left(1-0.19p_{crit-AgCl}\right)\cdot C_{OH^-} - 1.3\times10^{-4}p_{crit-AgCl} + 1.12\times10^{-6}\left(1-p_{crit-AgCl}\right)}{\left(1-p_{crit-AgCl}\right)\cdot C_{Ag^+} + 1.3\times10^{-4}p_{crit-AgCl} - 1.12\times10^{-6}\left(1-p_{crit-AgCl}\right)}. \qquad (25)$$

It can be seen from Eq. (25) that critical R_2 at $P_{crit\text{-}AgCl}$ increases with the increase of C_{OH^-} and with the decrease of C_{Ag^+}. When $P_{crit\text{-}AgCl} = 0.65$ are used in Eq. (25), then:

$$R_{2-crit} \approx 2.57C_{OH^-} / C_{Ag^+} - 0.00252. \qquad (26)$$

Considering the range of $C_{OH}^{-} = 0.01$–0.6 mol/L and $C_{Ag}^{+} = 0.035$–0.5 mol/L, Eq. (26) can be written as Eq. (27):

$$R_{2-crit} \approx 2.57C_{OH^-} / C_{Ag^+}. \qquad (27)$$

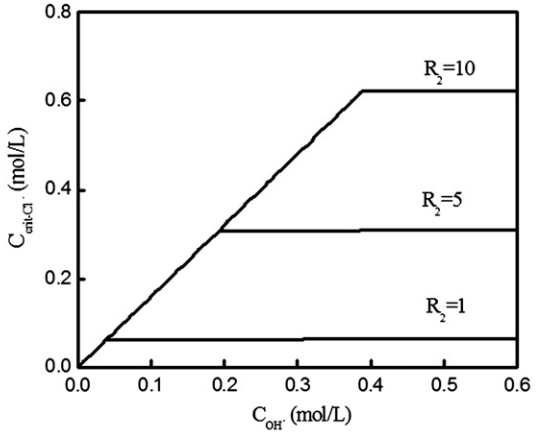

Fig. 7. Relationship between $C_{crit\text{-}Cl^-}$ and C_{OH^-} in case of 0.1 mol/L $AgNO_3$ solution.

Therefore, $R_{2\text{-}crit}$ at $P_{crit\text{-}AgCl}$ linearly increases with the increase of C_{OH}^-. Based on Eqs. (15), (20) and (27), Eq. (28) can be obtained.

$$C_{\ crit-Cl} = \begin{cases} 1.6C_{OH^-},R_2 \geq 2.57C_{OH^-} / C_{Ag^+}(a) \\ 0.00695C_{OH^-} + 0.608C_{Ag^+}R_2,\ R_2 < 2.57C_{OH^-} / C_{Ag^+}(b). \end{cases} \quad (28)$$

Based on Eq. (28), when concentration of $AgNO_3$ solution is 0.1 mol/L, the relationship between $C_{crit\text{-}Cl^-}$ and C_{OH^-} is plotted in Fig. 7. As can be seen from the figure, no matter what R_2 is, curves with similar trends are obtained. Within the whole range of OH^- ion concentrations, the smaller the R_2 is, the lesser the $C_{crit\text{-}Cl^-}$ changes. When pore solution volumes of specimens are the same, the lesser the volume of sprayed $AgNO_3$ solution is, the smaller the $C_{crit\text{-}Cl^-}$ range is. To obtain a smaller $C_{crit\text{-}Cl^-}$ range, sprayed amount of $AgNO_3$ solution should be as less as possible, but the surface of cement-based materials must be completely wetted by $AgNO_3$ solution.

4.2. Determination of chloride concentration at the color change boundary

4.2.1. In the case of $R_2 > R_{2\text{-}crit}$

Based on discussions in Section 3, in the case of $AgNO_3$ amount is enough to react with all Cl^- and OH^- ion at the color change boundary, $P_{crit\text{-}AgCl}$ is 0.65, then R_1 is 1.6. Considering OH^- concentration in concrete, a range of 0.02–0.6 mol/L was used for the calculation of the chloride concentration at color change boundary of concrete. According to Eq. 28(a), chloride concentration C_d of pore solution at color change boundary changes in range of 0.03–0.96 mol/L. This indicates that free chloride concentration at the color change boundary of concrete does change in a wide range. This explains the range of 0.071–0.714 mol/L, as measured by Yuan [15].

Many researchers have expressed chloride concentration at color change boundary of $AgNO_3$ colorimetric measurement by mass of the binder (C_{bd}) for the purpose of simple chloride measurement. In this study, C_{bd} is calculated according to Eq. (29) and listed in Table 7. From Table 7, it can be seen that C_{bd} changes from 0.011% to 2.27% by mass of the binder. This is very similar to the range of 0.01%–1.69% as reported in published papers [4–6,12,15,17].

$$C_{bd} = 35.5P \times 1.6C_{OH^-} \times 100\% / M_{binder}. \quad (29)$$

4.2.2. In the case of $R_2 < R_{2\text{-}crit}$

Based on Eq. (28b), when $C_{Ag^+} = 0.1$ mol/L, since the constant 0.00695 for C_{OH^-} is about 1/10 of the constant 0.0608 for R_2, the effect of OH^- concentration on C_d could be ignored. Therefore, it can be seen from Eq. (28) that chloride concentration (in pore solution) at the color change boundary is mainly controlled by R_2. R_2 depends on volume ratio of $AgNO_3$ and pore solution taking part in the colorimetric reaction. This means that a proper amount of sprayed $AgNO_3$ solution maybe obtain similar chloride concentration at color change boundary of concentration with similar content of pore solution.

Ostuki et al. [4] found that water soluble chloride contents in cement paste, mortar and concrete were the same, which was approximately 0.15% by mass of cement. They used ordinary Portland cement (OPC) for their colorimetric experiments and 0.1 mol/L $AgNO_3$ solution as colorimetric indicator. The OH^- concentration in pore solution of hardened OPC paste is assumed as 0.6 mol/L. According to Eq. (27), $R_{2\text{-}crit} = 25.7 \times 0.6 = 15.4$. This means that when $R_2 < 15.4$, C_{bd} can be calculated according to Eq. (30).

$$C_{bd} = 35.5P\left(0.00695C_{OH^-} + 0.608R_2 / C_{Ag^+}\right) \times 100 / M_{binder}. \quad (30)$$

Assuming that R_2 changes from 1 to 10, binder content is 400 kg/m^3 and bulk density of concrete is 2400 kg/m^3, C_{bd} was calculated according to Eq. (30) and its contour was given in Fig. 8. It can be seen from the figure that, when R_2 is less than 6, even if the pore solution content changes from 4 to 16% (by volume of concrete), C_{pd} can be equal to 0.132%. This maybe explain why Ostuki et al. [4] found that water soluble chloride contents in cement paste, mortar and concrete were the same — about 0.15% by the mass of binder.

4.3. Factors influencing chloride concentration at the color change boundary

To concrete specimens exposed to chloride environment, from exposed surface to the chloride penetration front, OH^- concentration distribution in pore solution of hardened concrete increases slightly owing to leaching out and electrical migration of OH^- [26]. On the other hand, Cl^- gradually decreases with depth. Therefore, the concentration ratio of Cl^-/OH^- (R_2) in pore solution of concrete gradually decreases. For specimens with a given alkalinity, in the case of all Cl^- and OH^- can't completely react with $AgNO_3$, decreased volume and concentrations of sprayed $AgNO_3$ solution can result in lower R_2 detected, which means a lower chloride concentration at the color change boundary. However, higher volume and concentration of sprayed $AgNO_3$ solution does not always produce higher chloride concentration at the color change boundary. This is because when all OH^- and Cl^- ions react with $AgNO_3$ solution, R_2 at color change boundary reach $R_{2\text{-}crit}$ and doesn't change any more with increase of volume and concentration of sprayed $AgNO_3$ solution. In this situation, the chloride concentration at the

Table 7
Calculated chloride concentration at color change boundary during $AgNO_3$ colorimetric measurement for concrete.

	Parameters for the calculation of $C_{crit\ Cl^-}$			
	Bulk density	Pore solution content (% by volume of specimen)	Binder content	OH^- concentration
Assumed range	2400 kg/m^3	5–20%	300–500 kg/m^3	0.02–0.6 mol/L
Calculated C_{bd}		0.011%–2.27% by mass of binder		

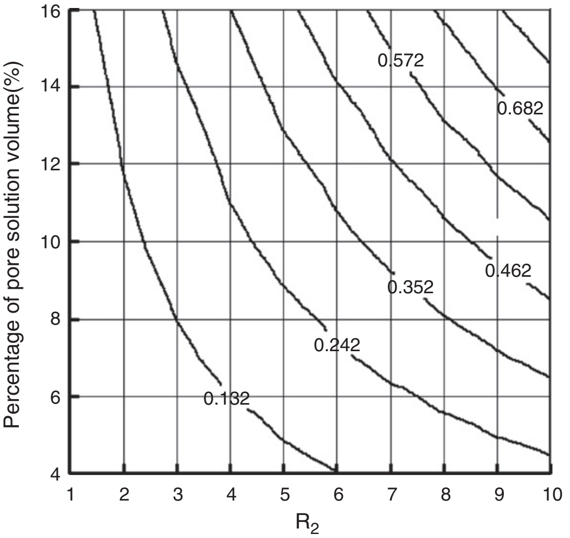

Fig. 8. C_{bd} contour as a function of R_2 and Porosity.

boundary doesn't change with concentration and volume of sprayed $AgNO_3$ solution.

Based on above discussions, in association with Eqs. (15) and (20), it can be seen that C_{OH^-}, C_{Ag^+}, R_2 may affect $C_{crit\text{-}Cl^-}$. R_2 depends on volume of $AgNO_3$ solution and pore solution taking part in the colorimetric reactions. This means that alkalinity of concrete, concentration and volume of sprayed $AgNO_3$ solution and pore solution content may influence the chloride concentration at the color change boundary, the effect trends of these factors on C_d are summarized in Table 8.

It can be found from above discussions that both calculated and measured C_d change in a wide range. However, a single value for C_d is used for the calculation of D_{nssm} in NT Build 492 [9], which could produce a large error. A small C_d range can be obtained if the amount of sprayed amount of $AgNO_3$ is properly controlled during the $AgNO_3$ colorimetric applications.

5. Conclusions

(1) $AgNO_3$ colorimetric measurement of cement-based materials can be implemented owing to chemical reactions between Ag^+, Cl^- and OH^- ions, which results in the formation of AgCl and Ag_2O. When the mass ratio of AgCl to precipitated AgCl + Ag_2O reaches $P_{crit\text{-}AgCl}$, a color change boundary appears.

(2) Calculated range of $C_{crit\text{-}Cl^-}$ is between 0.03 and 0.96 mol/L (in pore solution), or 0.011–2.27% by the mass of binder. This is in agreement with results in publications, 0.01 to 1.69% by the mass of binder or 0.071–0.714 mol/L in pore solution.

(3) Based on calculated results, it can be deduced that alkalinity of concrete, concentration and volume of sprayed $AgNO_3$ solution, and volume of pore solution have effects on measured chloride concentration at the color change boundary.

(4) Both calculated and measured C_d change in a wide range. However, a single value for C_d is used for the calculation of D_{nssm} in NT Build 492, which could produce a large error. A small C_d range can be obtained if the amount of sprayed amount of $AgNO_3$ is properly controlled during the $AgNO_3$ colorimetric applications.

Table 8
Factors influencing chloride concentration at the color change boundary.

Factors	Trend of the effect	
	Sufficient $AgNO_3$ solution	Insufficient $AgNO_3$ solution
Alkalinity of concrete↑	C_d ↑	Little effect
Concentration of $AgNO_3$ solution ↑	No effect	C_d ↑
Volume of $AgNO_3$ solution ↑	No effect	C_d ↑
Volume of pore solution ↑	No effect	C_d ↓

Acknowledgment

Financial supports from the National Natural Science Foundation of China (51072050) and Xiamen University of Science and Technology (3502Z20103042) Chinese National 973 Program are greatly appreciated.

References

[1] M. Collepardi, A. Marcialis, R. Turriziani, Kinetics of penetration of chloride ions into concrete (in Italian), Il Cemento 67 (1970) 157–164.
[2] M. Maultzsch, Concrete related effects on chloride diffusion (in German) BAMAmts- und. Mitteilungsblatt, Contribution to Int. Coll. Chloride Corrosion, Vienna 13 (3) (Feb. 22–23, 1983) 387–389.
[3] M. Collepardi, A. Marcialis, R. Turriziani, Penetration of chloride ions in cement pastes and in concretes, J. Am. Cer. Soc. 55 (10) (1972) 534–535.
[4] N. Otsuki, S. Nagataki, K. Nakashita, Evaluation of $AgNO_3$ solution spray method for measurement of chloride penetration into hardened cementitious matrix materials, ACI Mater. J. 89 (6) (1992) 587–592.
[5] V. Baroghel-Bouny, P. Belin, M. Maultzsch, D. Henry, $AgNO_3$ spray tests: advantages, weaknesses, and various applications to quantify chloride ingress into concrete. PartI: non-steady-state diffusion tests and exposure to natural conditions, Mat. Struc. J. 40 (8) (2007) 759–781.
[6] V. Baroghel-Bouny, P. Belin, M. Maultzsch, D. Henry, $AgNO_3$ spray tests: advantages, weaknesses, and various applications to quantify chloride ingress into concrete. PartII: non-steady-state migration tests and chloride diffusion coefficients, Mat. Struc. J. 40 (8) (2007) 783–799.
[7] F. He, C. Shi, Q. Yuan, et al., A Study on factors influencing chloride concentration at color change boundary of concrete using $AgNO_3$ colorimetric method [in Chinese], J. Chinese Ceram. Soc. 36 (7) (2008) 890–895.
[8] G. Chen, W. Li, P. Wang, Penetration depth and concentration distraction of chloride ions into cement mortar (in Chinese), Journal of Tong Ji University 24 (3) (1996) 19–24.
[9] NT Build 492, Nordtest method, concrete, mortar and cement-based repair materials: chloride migration coefficient from non-steady-state migration experiments, Espoo, Finland, 1999.
[10] C. Chiang, C. Yang, Relation between the diffusion characteristic of concrete from salt ponding test and accelerated chloride migration test, Mater. Chem. Phys. 106 (2–3) (2007) 240–246.
[11] L. Tang, Electrically accelerated methods for determining chloride diffusivity in concrete — current development, Mag. Concr. Res. 48 (176) (1996) 173–179.
[12] E. Meck, V. Sirivivatnanon, Field indicator of chloride penetration depth, Cem. Concr. Res. 33 (8) (1999) 1113–1117.
[13] V. Baroghel-Bouny, T.Q. Nguyen, M. Thiery, P. Dangla, P. Belin, Evaluation and prediction of reinforced concrete durability by means of durability indicators. Part I: new performance-based approach, in: K. Kovler (Ed.), Proceedings of international RILEM-JCI seminar on concrete durability and service life planning “ConcreteLife '06”, RILEM Publications, Bagneux, PRO 46, Ein-Bokek, Dead Sea, Israel, March 14–16, 2006, pp. 259–269.
[14] Stanish K. The migration of chloride ions in concrete. [Ph.D. dissertation]. Canada: Department of Civil Engineering, University of Toronto, 2002.
[15] Yuan Q. Fundamental studies on test methods for transport of chloride ions in cementitious materials. [Ph.D. dissertation]. Belgium: Department of Structural Engineering, Gent University, 2009.
[16] M. Collepardi, Quick method to determine free and bound chlorides in concrete, in: L.O. Nilsson, J.P. Ollivier (Eds.), Proceedings of the International RILEM Workshop-Chloride Penetration Into Concrete. Paris, 1995.
[17] V. Sirivivatnanon, R. Khatri, Chloride penetration resistance of concrete, presented to Concrete, Institute of Australia Conference Getting a Lifetime out of Concrete Structures. Brisbane, Australia, October 1998.
[18] C. Andrade, M. Castellote, C. Alonso, C. Gonzalez, Relation between colorimetric chloride penetration depth and charge passed in migration tests of the type of standard ASTM C1202-91, Cem. Concr. Res. 29 (3) (1999) 417–421.
[19] D. McPolin, P.A.M. Basheer, A.E. Long, K.T.V. Grattan, T. Sun, Obtaining progressive chloride profiles in cementitious materials, Constr. Build. Mater. 19 (9) (2005) 666–673.
[20] C. Alonso, C. Andrade, M. Castellote, P. Castro, Chloride threshold values to depassivate reinforcing bars embedded in a standardized OPC mortar, Cem. Concr. Res. 30 (2000) 1047–1055.
[21] C. Shi, J.A. Stegemann, R. Caldwell, Effect of supplementary cementing materials on the rapid chloride permeability test (AASHTO T 277 and ASTM C1202) results, ACI Mater. J. 95 (4) (1998) 389–394.

[22] Q. Yuan, C. Shi, F. He, G.D. Schutter, A. Audenaert, K. Zheng, Effect of hydroxyl ions on chloride penetration depth measurement using the colorimetric method, Cem. Concr. Res. 38 (10) (2008) 1177–1180.
[23] C.L. Page, O. Vennesl, Pore solution composition and chloride binding capacity of silica fume cement pastes, Mater. Struct. 16 (1) (1983) 19–25.
[24] R.K. Dhir, M.A.K. El-Mohr, T.D. Dyer, Developing chloride resisting concrete using PFA, Cem. Concr. Res. 27 (11) (1997) 1633–1639.
[25] C. Arya, N.R. Buenfeld, J.B. Newman, Factors influencing chloride binding in concrete, Cem. Concr. Res. 20 (2) (1990) 291–300.
[26] H.W. Song, C.H. Lee, K.Y. Ann, Factors influencing chloride transport in concrete structures exposed to marine environments, Cem. Concr. Compos. 30 (2) (2008) 113–121.